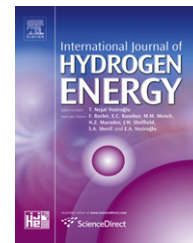


Available at www.sciencedirect.comjournal homepage: www.elsevier.com/locate/he

Comparative study of H-atom location, electronic and chemical bonding in ideal and vacancy containing-FCC iron

D. Rey Saravia^a, A. Juan^{a,*}, G. Brizuela^a, S. Simonetti^{a,b,1}

^a Departamento de Física, Universidad Nacional del Sur, Av. Alem 1253, 8000 Bahía, Blanca, Argentina

^b Research Center in Theoretical and Applied Mechanics, Universidad Tecnológica Nacional, 11 de Abril 461, 8000 Bahía Blanca, Argentina

ARTICLE INFO

Article history:

Received 15 May 2009

Received in revised form

30 July 2009

Accepted 6 August 2009

Available online 27 August 2009

Keywords:

Hydrogen

Iron

Vacancy

Modeling and simulation

Electronic structure

ABSTRACT

We studied one of the aspects of iron embrittlement in an FCC lattice with a vacancy in the presence of hydrogen as an impurity. The energy calculations were performed using the ASED method (Atom Superposition and Electron Delocalization). The electronic structures were analyzed by the YAeHMOP program (extended Hückel Molecular Orbital Package). H in bulk FCC iron prefers octahedral sites while in the presence of a vacancy it is located near the defect in a position shifted from the center of the hole. The formed Fe–H bond makes the Fe–Fe bonds first neighbors to the vacancy 28% weaker with respect to the H-free structure.

© 2009 Professor T. Nejat Veziroglu. Published by Elsevier Ltd. All rights reserved.

1. Introduction

Fuel cell vehicles have been identified as the personal transportation technology of the future because of their high efficiency and very low emissions. To achieve the goal of road-ready fuel cell vehicles, great strides must be made in the development of fuel cells, hydrogen production, and hydrogen storage technologies that include metal–H interaction studies and safety considerations.

Pure bulk face centered cubic (FCC) iron in the presence of hydrogen atmospheres undergoes severe embrittlement due to small amounts of absorbed hydrogen. Severe embrittlement, rupture under stress and corrosion due to hydrogen interaction have been observed in a large number of metals and alloys including high-strength steels [1–4]. Scientists and technologists have studied hydrogen in bulk metals for many

years [5–8]. Engineers have intended to solve technological problems such as protecting structure from hydrogen embrittlement [9–11], transporting of liquid hydrocarbons in the presence of hydrogen at high temperatures [12], storing hydrogen fuel at high densities without the danger of high pressures [13–15], and designing nuclear fusion reactors [16].

The interactions of hydrogen with lattice imperfections determine the influence of this impurity on the properties of solids. Interesting observations and results on vacancy contributions to hydrogen embrittlement and hydrogen-induced degradation of the mechanical properties of metals, especially in steels, have been recently investigated [17]. On the other hand, the role of vacancies in the hydrogen storage properties of Prussian blue analogues has been studied by Kaye and Long [18]. Wen et al. have investigated the H interaction with ideal and vacancy containing-BCC Fe surfaces.

* Corresponding author. Tel.: +54 291 4595141; fax: +54 291 4595142.

E-mail address: cajuan@criba.edu.ar (A. Juan).

¹ Tel.: +54 291 4555220.

The results revealed that H accumulates at the tip of the crack inducing embrittlement [19].

According to Hu et al., hydrogen embrittlement in a single crystal of α -Fe could be qualitatively described as a process of cavity nucleation, cavity linkage, and finally, fracture [20]. Baranov et al. studying BCC and FCC metals with hydrogen impurities concluded that cracks do not propagate in pure metals [21].

Juan and Hoffmann have studied H absorption, both in ideal and vacancy containing-BCC bulk Fe [22]. These authors observed that hydrogen prefers tetrahedral (t) interstitial sites in BCC bulk Fe and the vacancies could act as trapping centers for hydrogen. Furthermore, they concluded that H in BCC Fe sits near the vacancy. Juan et al. have studied Fe–H interaction and electronic structure of an H-vacancy bonding in BCC Fe [23] and have found that the hydrogen harmful effect is limited to the Fe first neighboring atoms.

Minot and Demangeat have studied the electronic structure of Fe–H bond in BCC and HCP phases [24]. Their results indicate that the formation of the bond is endothermic and that the preferred location of H in both lattice structures is tetrahedral interstitial sites.

The hydrogen and deuterium effect at high pressures, in AISI 304 and AISI 310 stainless steels, have been investigated by Rietveld neutron diffraction. The analysis shows that H-atoms occupy only octahedral interstitial sites in both steels [25].

Jiang and Carter have reported periodic spin-polarized density functional theory (DFT) predictions on hydrogen adsorption, absorption, dissolution and diffusion in ferromagnetic BCC iron. The authors have found that H prefers to stay on the Fe surface instead of on sub-surfaces or in the bulk. Hydrogen dissolution in bulk Fe is predicted to be endothermic, with hydrogen occupying tetrahedral interstitial sites over a wide range of concentrations. This is consistent with the well known low solubility of H in pure Fe [26]. It is also well known that hydrogen prefers the tetrahedral site location in BCC Fe and the octahedral one in FCC Fe [27,28].

Itsumi and Ellis have investigated the electronic properties of BCC Fe [29]. They found that Fe–Fe bond of the nearest neighbor atoms is weakened due to the presence of H. Hydrogen in combination with a vacancy occupies a position displaced from the center of the octahedral site toward the vacancy.

The total structural energy per primitive unit cell, the density of electron states, the spatial distribution of electrons and the elastic modulus in FCC Fe–H solid solutions were studied using the density functional theory and Wien2k program package. The density of conduction electrons is higher in the vicinity of hydrogen atoms, which suggests that the latter migrates over the crystal lattice surrounded by the clouds of conduction electrons. It is concluded that hydrogen-induced brittleness of austenitic steels can be satisfactorily interpreted in terms of the hydrogen effect on the electronic structure [27].

In this work, theoretical studies are performed to understand the effect of hydrogen on the embrittlement process of FCC Fe. A relation is found between H absorption in ideal bulk FCC iron and H-atom location in an FCC Fe lattice containing a vacancy.

2. FCC Fe clusters and computational method

FCC packing in metals has a three-layer sequence ABCABC, with the (111) being the most compact plane. When one layer of spheres is placed on top of another one, two types of holes are formed depending on the number of spheres surrounding them; namely, tetrahedral and the octahedral. For a given number of spheres, there are the same number of octahedral holes and twice the number of tetrahedral ones. The octahedral holes are bigger than the tetrahedral ones. The ideal FCC lattice structure was represented by a cluster of 180 metallic atoms distributed over five closed packed planes, each one formed by 36 Fe atoms. The selected geometry of each plane is an equilateral triangle. The distance between planes is 2.074 Å. The reference plane is the central one, which is also taken as the co-ordinate origin. All the calculations were performed at the center of the cluster, in order to avoid border effects. As a second step, we changed the starting ideal FCC structure introducing a vacancy at the cluster center (179 atoms + 1 vacancy) (see Fig. 1(a)). We followed the same procedure, used the same parameter sets and then we compared the results of H introduction into the imperfect and ideal Fe structure. The analyses of the theoretical results were made from the energy contour plots corresponding to the H–Fe interaction covering all the ($\bar{1}\bar{1}0$) planes at steps of 0.05 Å. Once the most stable location for the hydrogen was found, the chemical bond and the electronic structure of the Fe–H and Fe–Fe interactions were computed, before and after H interaction, in the ideal and defect-containing FCC iron structures. The calculations were performed using the Atom Superposition and Electron Delocalization (ASED) method [30–33] and the electronic structure and bonding determined using the Yet Another extended Hückel Molecular Orbital Package (YAeHMOP) [34]. These semiempirical methods were chosen due to the size of the system under study and because both use experimental ionization potentials as input parameters and can provide useful information about the electronic structure and bonding of H-atom interactions in a transition metal matrix. A more detailed description is given in ref. [23].

The adiabatic total energy values were computed as the difference between the electronic energy (E) of the system when the H-atom was at finite distance within the bulk of Fe and the same energy when the H-atom was far away from the solid.

The “hydrogen atom absorption energy” can be expressed as:

$$\Delta E_{\text{total}} = E(\text{Fe}_n - \text{H}) - E(\text{Fe}_n) - E(\text{H}) + E_{\text{repulsion}} \quad (1)$$

where n is the number of Fe atoms in the cluster. For the ideal FCC structure of Fe, n is equal to 180. In the one containing a vacancy, n is equal to 179. The repulsive energy was computed by a summation of pair wise repulsive electrostatic energy terms. To understand all the interactions we used the concept of density of states (DOS) and crystal orbital overlap population (COOP) curves. The DOS curve is a plot of the number of orbitals per unit volume and per unit

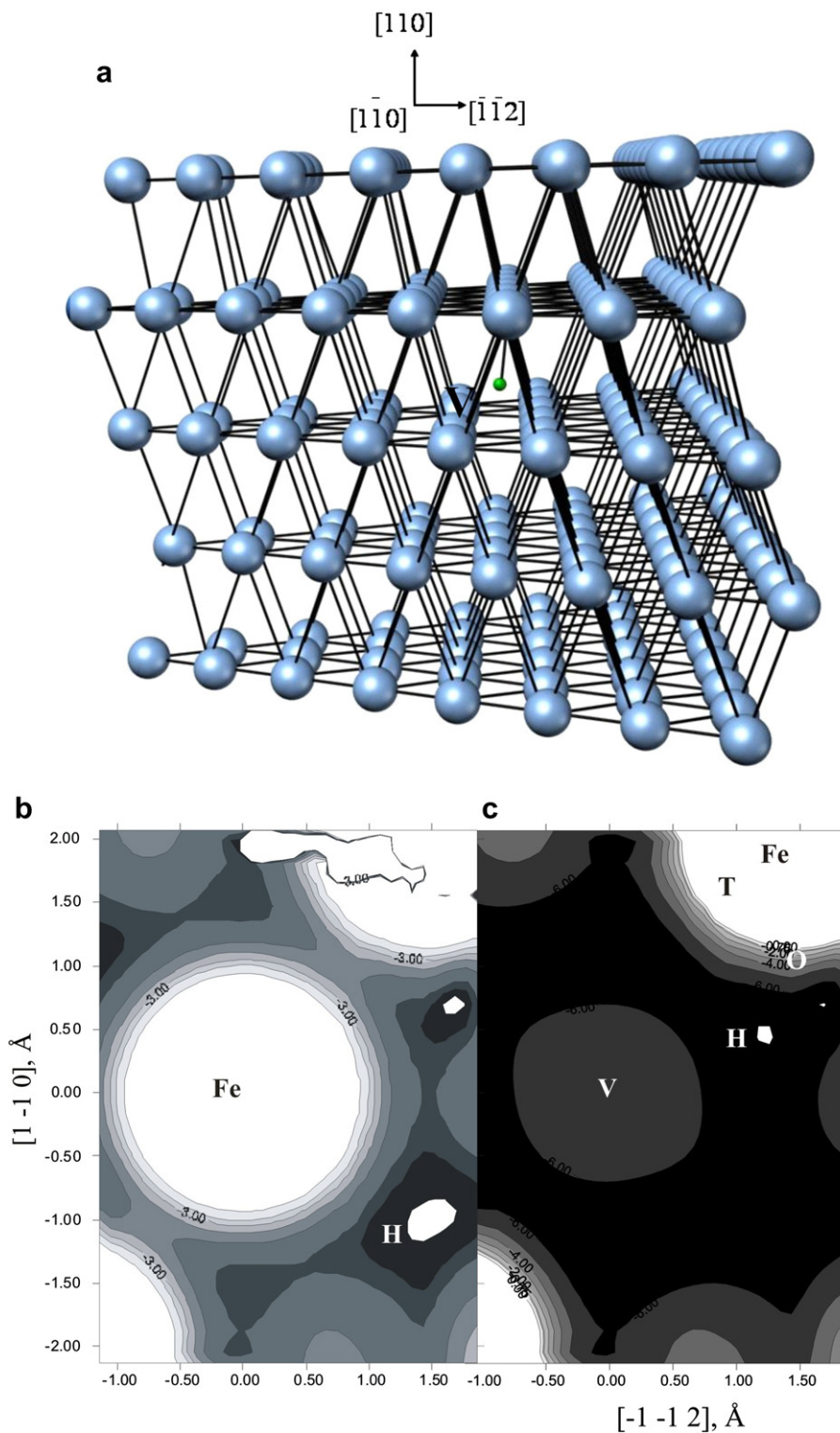


Fig. 1 – (a) A schematic view of the $\text{Fe}_{179+\text{V}-\text{H}}$ cluster. (b) Energy contour lines for the $\text{Fe}_{180-\text{H}}$ system. (c) Energy contour lines for the $\text{Fe}_{179+\text{V}-\text{H}}$ system. Octahedral (O) and tetrahedral (T) sites are indicated.

energy. The COOP curve is a plot of the overlap population weighted DOS vs. energy. The integration of the COOP curve up to the Fermi level (E_f) gives the total overlap population of the bond specified and it is a measure of the bond strength.

Recently we have used the ASED–YAHeMOP methodology for the study of H–Fe interactions in BCC and FCC structures [23,35–37]. We have also compared our ASED results with DFT calculations in Mg–Ni hydrides and multiple H-atoms interactions in Pd dislocations [38,39].

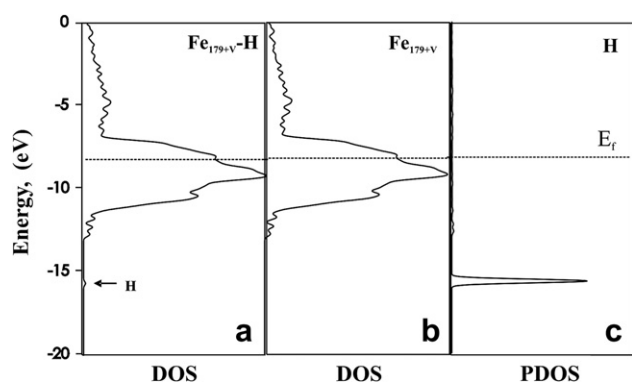


Fig. 2 – (a) Total DOS for the $\text{Fe}_{179+\text{V}}\text{-H}$ cluster. (b) Total DOS for the $\text{Fe}_{179+\text{V}}$ cluster. (c) Projected DOS over the H-atom in the $\text{Fe}_{179+\text{V}}\text{-H}$.

3. Results and discussion

3.1. Hydrogen atom location in the FCC Fe clusters

We calculated the energy of the system in order to localize the H-atom inside the ideal Fe cluster, having the most stable energy at -6.52 eV (see Fig. 1(b)). This minimum was found at 1.741 Å from the Fe first neighboring atom. This location in the FCC structure corresponds to an octahedral hole. Then, we performed the calculation for an H-atom inside the cluster containing the vacancy. The minimum energy value was found to be -6.72 eV at 1.617 Å distance from the closest Fe atom and at 1.340 Å from the center of the vacancy. Fig. 1(a) and (c) show the plots when H is located near the vacancy. Juan and Hoffmann have reported in the case of H on a BCC Fe (110) surface, an Fe–H distance of 1.64 Å [22]. Also, a minimum Fe–H distance between 1.4 Å and 1.7 Å was found for a vacancy containing-BCC Fe [28] while an Fe–H distance of 1.79 Å was reported for an FCC Fe stacking fault [36].

3.2. The electronic structure of the Fe–H systems

The density of states (DOS) of the ideal Fe_{180} structure containing the H-atom (not shown here) is mainly due to the Fe atoms. It is very similar to that obtained for the Fe cluster without H, except for a small peak located at -16.5 eV. This peak appears below the Fe d band and belongs to the H states after the Fe–H interaction is established. A narrow band at the d states between -12 and -7 eV is formed, while the s and p states are scattered and penetrate the d band. The Fermi energy value is -8.201 eV.

The density of states (DOS) for the $\text{Fe}_{179+\text{V}}$ system is similar to that of the Fe_{180} system, if we compare, on the one side the isolated systems and, on the other side, the systems containing H. This is because the DOS changes are negligible when only one vacancy and only one H-atom are present. The (E_f) value for the $\text{Fe}_{179+\text{V}}\text{-H}$ system is -8.205 eV. The DOS plots for the $\text{Fe}_{179+\text{V}}$ system with and without H are shown in Fig. 2. The interstitial H-atom extended its influence only to the Fe first neighbors.

After H introduction, the s orbital population from the closest Fe atom has a 9% reduction and simultaneously the population of the p and the d orbitals decreases by 8% and 3%, respectively. These facts indicate that 4s and 4p orbitals of the closest Fe atoms contribute to the main H–Fe interaction. A loss of 0.179 e charge between Fe atoms close to the hydrogen was also observed, while the H-atom gained a -0.273 e charge (see Table 1). The H introduction into the $\text{Fe}_{179+\text{V}}$ system also affects the Fe first neighbors, changing its electronic density. The s orbital from the Fe atoms nearest to the vacancy decreases its orbital population to about 12% and, the p and d orbital population decrease by 2% and 3%, respectively, indicating the main contribution of the 4s orbitals to the Fe–H interaction. A 0.256 e charge variation takes place between the H closest Fe atoms. The H presents a negative charge of -0.328 e and at the same time a positive charge is developed at the Fe first neighbors (see Table 1). The charge and electronic structure of Fe atoms second nearest neighbors are not affected by the presence of H. The

Table 1 – Electron orbital occupation and net charge for the H-atom and its nearest neighbors iron atoms. Fe–H and Fe–Fe distances and the respective bonds overlap population (OP).

Atom	Electron orbital occupation			Charge	Bond	Distance (Å)	OP
	s	p	d				
FCC Fe_{180}							
H	1.273		-0.273				
Fe	0.621	0.276	5.890	1.213	H–Fe	1.741	0.188
Fe_{nn}	0.628	0.274	5.989	1.110	Fe– Fe_{nn}	2.540	0.158
FCC $\text{Fe}_{179+\text{V}}$							
H	1.328		-0.328				
Fe	0.619	0.309	6.045	1.025	H–Fe	1.617	0.312
Fe_{nn}	0.685	0.293	6.069	0.953	Fe– Fe_{nn}	2.540	0.163

nn: nearest neighbor atom.

a OP for the same bond without H in the cluster.

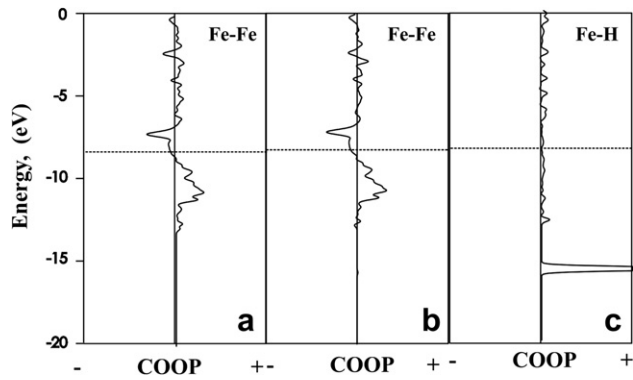


Fig. 3 – COOP curves for the Fe–Fe interaction (a) in the $\text{Fe}_{179+\text{V}}$ cluster and (b) in the $\text{Fe}_{179+\text{V}-\text{H}}$ cluster. (c) COOP curve for the Fe–H interaction in the $\text{Fe}_{179+\text{V}-\text{H}}$ cluster.

H effect is local and due to the size of the 1s orbital is unable to interact with other Fe atoms.

Norlander et al. established that in high electron density metals, the density decrease by defects and H impurities is more stable [40]. H-atoms also have their minimum energy off the defect-center, closer to metal atoms. In the case of the ideal Fe_{180} cluster (not shown here), the Fe–Fe overlap population decreases from 0.225 to 0.158 when hydrogen is absorbed. On the other hand, COOP curves for the $\text{Fe}_{179+\text{V}}$ cluster (see Fig. 3(a) and (b)) show that the Fe–Fe overlap population for the Fe atoms closest to hydrogen decreases 28% from 0.227 for the cluster without H to 0.163 for the cluster containing the H-atom. This reduction is lower than the one for the ideal cluster. For the Fe–H interactions in the ideal Fe_{180} cluster, most of the electronic states are filled; however, the anti-bonding states are pushed up over the Fe 3d band. The main interaction arises from the H 1s orbital interaction with the Fe 4s and 4p orbitals, with a small contribution coming from the Fe 3d. The computed Fe–H overlap population is 0.188.

The COOP curve of the Fe–H bond in the $\text{Fe}_{179+\text{V}}$ cluster (see Fig. 3(c)), shows that most of the bonding states are also filled and that the anti-bonding states are pushed up above the Fe 3d band. The peak at -16.5 eV is mainly due to the H1s–Fe 4s interaction. In both cases the peaks indicate a strong bonding interaction between H and Fe. Comparing both clusters, the Fe–H overlap population from the $\text{Fe}_{179+\text{V}}$ cluster is 0.312, which is much larger than in the ideal Fe_{180} cluster (0.188). Thus, the vacancy zone is the most favorable region for the H-atom location.

4. Conclusions

The most stable position for the H-atom, in both ideal FCC Fe and FCC Fe containing a vacancy, was determined. Using ASED calculations, we found that in an ideal bulk system the octahedral site is energetically favorable (as the experimental studies indicate); however, in the vacancy-containing system, the H-atom prefers the vacancy region and an off-center location. The Fe–H distance was also calculated and a good agreement, compared with literature data, was found. The

Fe–Fe interaction in the metallic matrix for both systems, before and after the hydrogen atom-introduction, was also analyzed. We observed a 28% weakening of the Fe–Fe metal bond in the neighborhood of the H-atom. This bond decohesion could be associated with the embrittlement due to H interaction.

Acknowledgements

Our work was supported by General Secretary of Science and Technology-Universidad Nacional del Sur, Department of Mechanical Engineering-Universidad Tecnológica Nacional, projects of scientific and technological research PICT 1186/2006 and 560/2007, CONICET (National Council of Scientific and Technical Researches of Argentina) and pluri-annual projects of research PIP 2009 CONICET. A. Juan, G. Brizuela and S. Simonetti are members of CONICET. We also thank useful reviewers suggestions.

REFERENCES

- [1] Chene J, Brass A. Hydrogen transport by mobile dislocations in nickel base superalloy single crystals. *Scr Mater* 1999;40: 537–42.
- [2] Brass A, Chene J. Rôle des interfaces et des dislocations sur la diffusion et le piégeage de l'hydrogène dans les matériaux métalliques. *J Physique IV* 1999;9:4–165.
- [3] Brass A, Chene J. Influence of deformation on the hydrogen behavior in iron and nickel base alloys: a review of experimental data. *Mater Sci Eng A* 1998;242:210–21.
- [4] Krom A, Koers R, Bakker A. Hydrogen transport near a blunting crack tip. *J Mech Phys Solids* 1999;47:971–92.
- [5] Oriani R. The diffusion and trapping of hydrogen in steel. *Acta Metall* 1970;18:147–57.
- [6] Kehr K. In: Alefeld, Völk J, editors. *Hydrogen in metals*. Springer series in materials sciences, vol. I. Berlin: Springer; 1978.
- [7] Kirchheim R. Solubility, diffusivity and trapping of hydrogen in dilute alloys. Deformed and amorphous metals-II. *Acta Metall* 1982;30:1069–78.
- [8] Kirchheim R, Hirth J. Stress and solubility for solutes with asymmetrical distortion fields. *Acta Metall* 1987;35:2899–903.
- [9] Oriani R. Hydrogen embrittlement of steels. *Ann Rev Mater Sci* 1978;8:327.
- [10] Moody N, Thompson A, editors. *Hydrogen effect on material behavior, the minerals*. Warrendale, PA: Metals and Materials Society; 1990.
- [11] Fukai Y. In: Gonser U, editor. *The metal hydrogen system*. Springer series in material sciences, vol. 21. Berlin: Springer; 1993.
- [12] Borruto A, Borruto T, Spada A. Hydrogen–steel interaction: hydrogen embrittlement in pipes for power former plant effluents. *Int J Hydrogen Energy* 1999;24:651.
- [13] Wiswall R. In: Alefeld G, Völk J, editors. *Hydrogen in metals*. Springer series in materials sciences, vol. II. Berlin: Springer; 1978.
- [14] Kirchheim R, Fromm E, Wicke E, editors. *Proceedings of the international symposium on metal-hydrogen systems: fundamentals and applications*, Z. Phys. Chem., N.F.; 1989. p. 163–4.
- [15] Sandrock G. In: Yürüm Y, editor. *Hydrogen energy system*. Netherlands: Kluwer; 1995.

- [16] Wilson KL, Pontau AE. The temperature dependence of deuterium trapping in fusion reactor materials. *J Nucl Mater* 1979;85–86(2):989–93.
- [17] Naguno M. Function of hydrogen in embrittlement of high-strength steels. *ISIJ Int* 2001;41:590–8.
- [18] Kaye S, Long J. The role of vacancies in the hydrogen storage properties of Prussian blue analogues. *Catal Today* 2007;120:311–6.
- [19] Wen M, Xu X, Fukuyama S, Yokogawa K. Embedded-atom-method functions for the body-centered-cubic iron and hydrogen. *J Mater Res* 2001;16:3496–502.
- [20] Hu Z, Fukuyama S, Yokogawa K, Okamoto S. Hydrogen embrittlement of a single crystal of iron on a nanometre scale at a crack tip by molecular dynamics. *Modell Simul Mater Sci Eng* 1999;7:541–51.
- [21] Baranow M, Drozdow A, Chudinov V, Bayankin V. Atomic mechanisms of microcrack propagation in pure and hydrogen-containing FCC and BCC metals. *Tech Phys* 2000;45:427–31.
- [22] Juan A, Hoffmann R. Hydrogen on the Fe(110) surface and near bulk BCC Fe vacancies: a comparative bonding study. *Surf Sci* 1999;421:1–16.
- [23] Juan A, Pistonesi C, Garcia A, Brizuela G. The electronic structure and bonding of a H–H pair in the vicinity of a BCC bulk vacancy. *Int J Hydrogen Energy* 2003;28:995–1004.
- [24] Minot C, Demangeat C. Hydrogen in iron, vanadium and FeV: heat of formation, lattice location and the hydrogen-metal bond. *J Less-Common Metals* 1987;130:285–91.
- [25] Hoelzela M, Danilkin S, Ehrenberga H, Toebbens D, Udovic T, Fuessa H, et al. Effects of high-pressure hydrogen charging on the structure of austenitic stainless steels. *Mater Sci Eng A* 2004;384:255–61.
- [26] Jiang D, Carter E. Diffusion of interstitial hydrogen into and through bcc Fe from first principles. *Phys Rev B* 2004;70:064102–11.
- [27] Teus S, Shivanyuk V, Shanina B, Gavriljuk V. Effect of hydrogen on electronic structure of fcc iron in relation to hydrogen embrittlement of austenitic steels. *Phys Stat Sol (a)* 2007;204(12):4249–58.
- [28] Simonetti S, Pistonesi C, Brizuela G, Juan A. The multiple hydrogen location near a α -Fe vacancy. *J Phys Chem Solids* 2005;66:1240–6.
- [29] Itsumi Y, Ellis D. Electronic bonding characteristics of hydrogen in BCC iron: part I. Interstitials. *J Mater Res* 1996;11:2206–13.
- [30] Hoffmann R, Lipscom W. Theory of polyhedral molecules. III. Population analyses and reactivities for the carboranes. *J Chem Phys* 1962;36:2179–89.
- [31] Hoffmann R. An extended Hückel theory. I. Hydrocarbons. *J Chem Phys* 1963;39:1397–412.
- [32] Whangbo M, Hoffmann R. The band structure of the tetracyanoplatinate chain. *J Am Chem Soc* 1978;100:6093–9.
- [33] Anderson A. Derivation of the extended Hückel method with correlations: one electron molecular orbital theory for energy level and structure determinations. *J Chem Phys* 1975;62:1187–8.
- [34] Landrum GA, Glassey WV. Yet another extended Hückel molecular orbital package (YAeHMOP). Cornell University. YAeHMOP is freely available on the world wide web at: <http://yaehmop.sourceforge.net/>; 2004.
- [35] Juan A, Moro L, Brizuela G, Pronsato E. The electronic structure and bonding of an hydrogen pair near a FCC Fe stacking fault. *Int J Hydrogen Energy* 2002;27:333–8.
- [36] Simonetti S, Moro L, Gonzalez NE, Brizuela G, Juan A. Quantum chemical study of C and H location in an fcc stacking fault. *Int J Hydrogen Energy* 2004;29:649–58.
- [37] Simonetti S, Moro L, Brizuela G, Juan A. The interaction of carbon and hydrogen in a α Fe divacancy. *Int J Hydrogen Energy* 2006;31:1318–25.
- [38] Jasen PV, González EA, Brizuela G, Nagel OA, González GA, Juan A. A theoretical study of the electronic structure and bonding of the monoclinic phase of Mg_2NiH_4 . *Int J Hydrogen Energy* 2007;32:4943–8.
- [39] Gesari SB, Pronsato ME, Juan A. Simulation of hydrogen trapping at defects in Pd. *Int J Hydrogen Energy* 2009;34:3511–8.
- [40] Nordlander P, Nørskov J, Besenbacher F. Trends in hydrogen heats of solution and vacancy trapping energies in transition metals. *J Phys F: Met Phys* 1986;16:1161–71.